Geometrically enhanced morphology-dependent resonances of a dielectric sphere

Abdullah Demir,[1] Emre Yüce,[2] Ali Serpengüzel,[3,*] and James A. Lock[4]

[1]Center for Research and Education in Optics and Lasers (CREOL), The College of Optics and Photonics, University of Central Florida, 4000 Central Florida Boulevard, Orlando, Florida 32816, USA

[2]Complex Photonic Systems (COPS), MESA+ Institute for Nanotechnology and Department of Science and Technology, University of Twente, P.O. Box 217, 7500 AE Enschede, The Netherlands

[3]Koç University, Microphotonics Research Laboratory, Department of Physics, Rumelifeneri Yolu, Sarıyer, Istanbul 34450, Turkey

[4]Department of Physics, Cleveland State University, Cleveland, Ohio 44115, USA

*Corresponding author: aserpenguzel@ku.edu.tr

Received 27 June 2011; revised 14 August 2011; accepted 16 August 2011; posted 17 August 2011 (Doc. ID 149841); published 16 December 2011

The effect that geometrical resonances of orbiting internally reflecting rays have on the morphology-dependent resonances of microspheres is investigated heuristically and numerically using generalized Lorenz–Mie theory. Angularly resolved off-axis Gaussian beam elastic scattering spectra are presented. The results obtained show that the elastic scattering intensity of morphology-dependent resonances is noticeably enhanced in the vicinity of the geometrical resonance scattering angles.

OCIS codes: 140.3945, 290.4020, 140.4780.

1. Introduction

Morphology-dependent resonances (MDRs) of microspheres [1] have quality factors that can be as large as 2×10^{10} [2]. These large-Q MDRs have found a variety of potential applications in microlasers [3], channel dropping [4], optical switching [5], ultrafine sensing [6], biomolecular agent detection [7], rotation detection [8], high-resolution spectroscopy [9], tunable filters [10], and Raman lasers [11]. In addition, silicon microspheres have been used in channel dropping [12] and have been considered for optoelectronic applications [13,14]. Recently, optical modulation in a silicon microsphere has been observed [15].

Among these applications, there has been much interest in optical miniature biosensors that utilize high-Q microsphere resonators [16]. These sensors have taken advantage of either the wavelength shift or the linewidth broadening of MDRs induced by the adsorption of biomolecules onto the surface of the microsphere [17]. While the wavelength shift of an MDR is caused either by a change in the refractive index or the size of the microsphere, linewidth broadening is frequently due to scattering losses that affect the cavity Q-factor [18]. Because of the importance of improving detector performance, increasing the sensitivity of these devices is crucial. Enhanced sensitivity of microsphere sensors can result from coating the microsphere with a high refractive index surface layer in order to increase the frequency shift sensitivity [19]. Ultrasensitive chemical sensors have been fabricated using film-coated microspheres [20].

In this paper, we report another enhancement of microsphere MDRs at specific and predictable scattering angles for special values of the refractive index corresponding to a geometrical resonance of the ray incident at the edge of the sphere. We find that geometrical-resonance-enhanced MDRs have a higher intensity in the vicinity of the resonant angles,

0003-6935/11/366652-05$15.00/0

leading to better sensitivity. In addition, this mechanism also provides an additional parameter, i.e., the angular dependence of the enhancement, for the detection and analysis of biological agents. Our approach thus differs from previous sensing enhancement methods leading to higher sensitivity, such as surface layer index change.

2. Optical Excitation of Microspheres

The excitation efficiency of MDRs by a focused beam can be made much higher than that for plane wave excitation if the center of the beam focus is suitably located [21]. Specifically, generalized Lorenz–Mie theory (GLMT) [22–24] predicts that a large coupling efficiency to the MDRs occurs when an off-axis Gaussian beam strongly illuminates the edge of the microsphere [25,–29]. One can qualitatively consider the Gaussian beam as a collection of parallel rays incident on the sphere surface. If one of the rays is incident at the angle θ_i and the sphere refractive index is m, the ray refracts at the angle θ_t according to Snell's law $\sin(\theta_i) = m\ \sin(\theta_t)$, where θ_t is the angle between the normal to the surface and the transmitted ray. Once inside the sphere, the transmitted ray repeatedly encounters the sphere surface and is partially transmitted and partially reflected each time. Let p denote the number of chords of the ray path inside the sphere before the ray exits and travels to the far zone. Like MDRs, geometrical resonances of the rays in the edge region also depend on both the sphere's radius and refractive index. The effect of geometrical resonances on the angular dependence of the MDR spectra then provides an additional experimental parameter with which to design input/output coupling to/from the microsphere.

3. Geometrical Resonances

Consider the family of geometrical rays that contributes to scattering by a microsphere after undergoing $p + 1$ interactions with the sphere surface. Given θ_i and p, the ray path inside the sphere, and thus the scattering angles, never repeat for most values of the refractive index. However, if the ray returns to the exact position, where it entered the sphere after $p + 1$ interactions with the sphere surface, and N orbits within the sphere, the number of scattering angles of the ray will be limited since the ray will always follow the same path during subsequent orbits. If this effect occurs with constructive interference as well, it is called a geometrical resonance [30,31] and can be used under certain circumstances to enhance MDRs at or near the scattering angles of the resonant ray. It should also be noted that geometrical resonances are also important in optical chaos when the scattering particle is deformed from its spherical shape [32,33]. These resonances occur only for specific values of the relative refractive index m. Consider for example the case of $N = 1$ and the edge ray with $\theta_i = \pi/2$. Then p becomes the number of internal chords per orbit. Two chords per orbit is physically impossible because 90° refraction of the edge ray requires an infinite refractive index. The first closed path thus has $p = 3$. The edge ray closed paths for $p = 3, 4, 5$ for $N = 1$ are shown in Fig. 1. Each interaction with the surface along the path is labeled by the index q, where $0 \le q \le p - 1$.

The ray paths inside the sphere in Fig. 1 can be geometrically considered as a sequence of triangles. The two base angles are equal to the critical angle for total internal reflection θ_c, and the vertex angle is $2\pi/p$. Then $2\theta_c + 2\pi/p = \pi$ and

$$\theta_c = \frac{\pi}{2}\left(1 - \frac{2}{p}\right). \tag{1}$$

Since $\theta_c = \sin^{-1}(1/m)$ in Eq. (1), the relation between m and p for a closed edge ray path after one orbit is

$$m = \frac{1}{\cos\left(\frac{\pi}{p}\right)}. \tag{2}$$

For a repeating ray path with $N = 1$, increasing p requires a lower relative refractive index, as is shown in Fig. 2. The cases of $p = 3, 4, 5$ give the refractive indices $m = 2.0, 1.414, 1.236$, respectively. A geometrical resonance will occur only if the ray path is closed *and* if the length of the ray path is an integer number of wavelengths M of light inside the sphere producing constructive interference of successive orbits. For edge ray incidence and $N = 1$, this occurs when

$$\lambda = \frac{2pa}{M}\tan\left(\frac{\pi}{p}\right), \tag{3}$$

where a is the sphere radius.

Equations (2) and (3) were derived assuming the incident ray just grazed the sphere surface with $\theta_i = \pi/2$. For an arbitrary incident ray, the right-hand side of Eqs. (2) and (3) should be multiplied by $\sin(\theta_i)$. Since the sine function is slowly varying in the vicinity of $\theta_i = \pi/2$, Eqs. (2) and (3) are a good approximation to the geometrical resonance condition for rays incident both at the edge of the sphere and in the vicinity of the edge.

The parameter space, i.e., the wavelength of the incident light and the scattering angle, for a sphere with $m = 2$ is pictorially illustrated in Fig. 3. The scattering angle theta is the angular deviation of

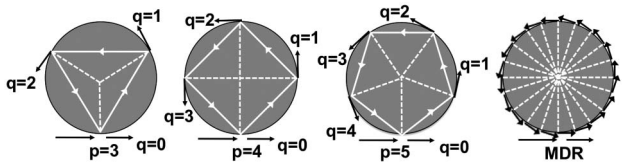

Fig. 1. Geometrical resonance formation geometries for $p = 3, 4, 5$ and $N = 1$. The black arrows outside the sphere denote the scattering angles of the geometrically resonant ray for $0 \le q \le p - 1$.

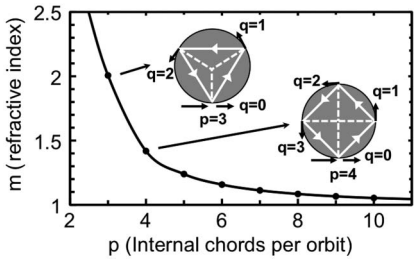

Fig. 2. Relative refractive index of the sphere for a geometrical resonance as a function of p for $N = 1$.

the scattered ray with respect to the direction of the incident ray, where positive theta corresponds to a counterclockwise deviation as in Fig. 1. The scattering angles of the geometrical resonance for the incident edge ray for $p = 3$ are $\theta = 0°$, $+120°$, $-120°$. These scattering angles are represented in Fig. 3 by three broad horizontal bands. The two narrow vertical lines in Fig. 3 represent the MDR wavelengths for partial wavenumbers $n + 1$ and n and radial mode number l. The rays corresponding to a relatively tightly focused Gaussian beam can be considered as having a certain degree of diffractive spreading. Therefore, the vertical lines are expected to be narrow due to high-Q factors of microsphere MDRs, while horizontal bands representing the geometrical resonances are expected to have a small but nonzero angular width that depends on the degree of focus of the incident beam. Although the conditions for a geometrical resonance of Eqs. (2) and (3) were derived in the context of ray theory, the resonance will be present as well in a wave treatment of scattering. The superposition of sharp MDRs and the geometrical resonances will then give rise to angularly localized enhanced intensities if the phase of the scattered MDR field and the phase of the scattered geometrical resonance field constructively interfere, or nearly so.

This should be a rather rare occurrence since the phase difference can randomly be anywhere between 0° and 180°. However, there is a mechanism that makes a 0° phase difference rather common. Consider the phase of a particular MDR as a fixed quantity. We mentioned that Eqs. (2) and (3) are nearly correct for rays that strike the sphere near the edge rather than only at the edge. But all those geometric resonances near the edge have slightly different path lengths from each other; thus they have different phases with respect to each other. One of these

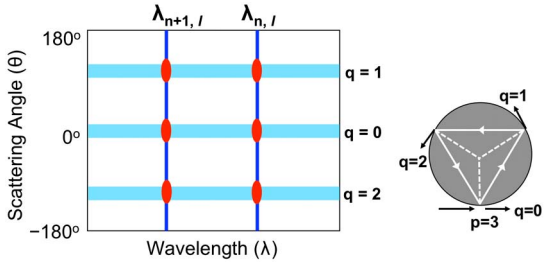

Fig. 3. (Color online) Expected spectral and scattering angle intensity distribution for $p = 3$ and $m = 2$.

phases is likely to be close to the phase of the MDR, giving the resonant enhancement. Said another way, the MDR phase selects the phase of one geometrical resonance out of all of them that have the same m and p values, but with different values of θ_i, for constructive interference and resonant enhancement.

4. Elastic Scattering Calculations

Numerical simulations based on GLMT for Gaussian beam illumination were made in order to explore the effects geometrical resonances on the MDRs of a microsphere. Focused off-axis illumination of a sphere was used to increase the MDR coupling strength and give higher power transfer into the microsphere. As an example, we studied the angularly resolved transverse magnetic (TM) and transverse electric (TE) elastic scattering spectra of a microsphere with radius $a = 10$ μm and refractive index $m = 2.0$ excited by a focused Gaussian beam, whose axis is parallel to the z axis and passes the sphere at the distance $b = +11.75$ μm from the origin and having field half-width $\omega_0 = 1.75$ μm in the beam focal plane. The focal plane contains the center of the microsphere, and the beam is incident just beyond the edge of the sphere. Classically, this corresponds to a ray that just misses striking the sphere. But in wave scattering, part of the amplitude tunnels through the centrifugal barrier surrounding the sphere and is transmitted inside. We considered the wavelength interval $\lambda = 1300$–1330 nm. The numerical computations used the localized model of the off-axis Gaussian beam polarized in the x direction, with the beam focal point longitudinal displacement $z_o = 0$, and having the beam confinement parameter $s = 0.12$ [34,35]. The details of the computational algorithm are also given in these references. TE scattering was computed when the beam was offset in the $+y$ direction, and TM scattering was computed when the beam was offset in the $+x$ direction. The calculations were performed using a wavelength resolution $\Delta\lambda = 30$ pm and the scattering angle resolution $\Delta\theta = 1°$.

Figures 4 and 5 show various details of the angularly resolved elastic scattering intensity as a function of wavelength and scattering angle for TM and TE polarizations, respectively. The TM and TE elastic light scattering intensity is shown in false color in decibels in Figs. 4(a) and 5(a). In order to illustrate the geometric resonance enhancement, the TM elastic light scattering intensity in decibels is also shown at scattering angles of 47° (off-geometric resonance) and 110° (on-geometric resonance) in Fig. 4(b). Similarly, the TE elastic light scattering intensity is shown at scattering angles of 47° (off-geometric resonance) and 96° (on-geometric resonance) in Fig. 5(b). In order to illustrate the MDR enhancement, the TM elastic light scattering intensity is shown at wavelengths of 1312 nm (off-MDR) and 1318 nm (on-MDR) in Fig. 4(c), and the TE elastic light scattering intensity is shown at wavelengths of 1320 nm (off-MDR) and 1326 nm (on-MDR) in Fig. 5(c).

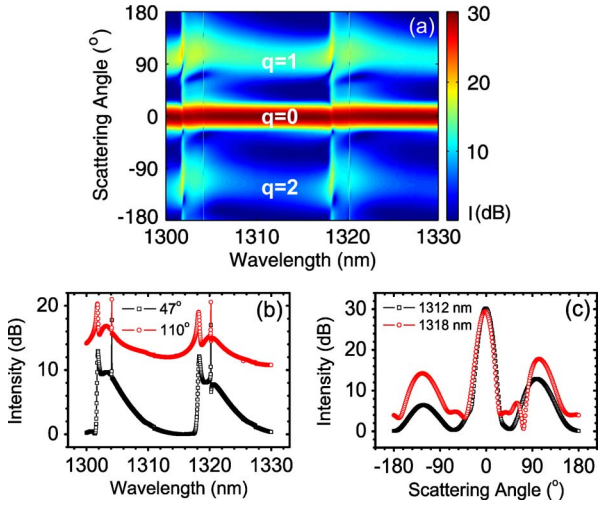

Fig. 4. (Color online) TM elastic light scattering intensity in decibels as (a) a false color image, (b) at scattering angles of 47° and 110°, and (c) at wavelengths of 1312 and 1318 nm.

The dominant features of Figs. 4(a) and 5(a) may be understood as follows. The large scattering enhancement near 0° is due to diffraction and electromagnetic surface waves for positive θ and grazing external reflection for negative θ. The $p = 2$ rainbow at $\theta = 180°$ is absent for both TE and TM scattering since it corresponds to $\theta_i = 0°$ for $m = 2$ and is not excited by edge incidence. On the other hand, the $p = 3$ rainbow at $\theta = -35.22°$ is visible in Fig. 5 for TE scattering as the shoulder on the forward scattering enhancement. For TM scattering, the $p = 3$ rainbow is absent due to the low value of the internal Fresnel reflection coefficient near the Brewster angle. The angularly broad geometrical resonance enhancements at $\theta = +120°$ and $\theta = -120°$ are clearly present in Figs. 4 and 5. The $\theta = +120°$ enhancement is stronger than the $\theta = -120°$ enhancement since the internally circulating light reaches the $\theta = 120°$ interface earlier in the ray path than it does for the $\theta = -120°$ interface. The geometrical resonances should have maximal constructive interference at $\lambda = 1299.0$, 1315.5, and 1332.3 nm for $M = 80, 79, 78$. In Fig. 4 for TM scattering, the peak enhancements at $\theta = +120°$ and $-120°$ are shifted with respect to these predictions by about +3.0 nm, and in Fig. 5 for TE incidence, they are shifted by about −4.4 nm. These relatively small shifts are likely due to the difference between the internal reflection phase shifts of the partial waves and the analogous geometrical rays since the sphere size parameter is $x = 2\pi a/\lambda = 48$, which is far below the short wavelength limit.

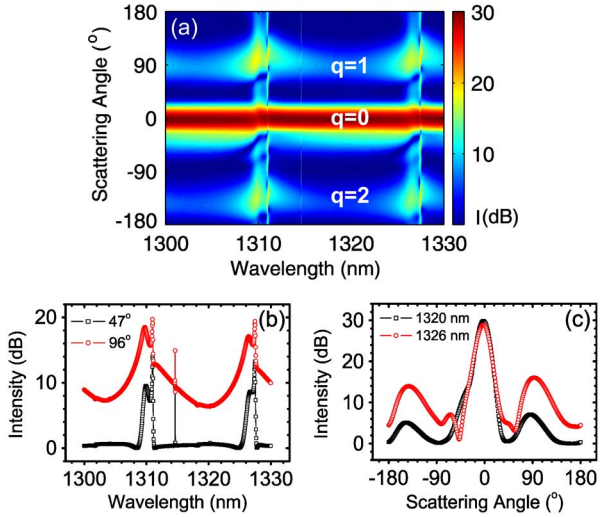

Fig. 5. (Color online) TE elastic light scattering intensity in decibels as (a) a false color image (b) at scattering angles of 47° and 96°, and (c) at wavelengths of 1320 and 1326 nm.

In Figs. 4 and 5, there are also two observable sets of MDRs with a mode spacing $\Delta\lambda \approx 16.4$ nm, whose Q-factors are in the range 10^3 to 10^4. For TM scattering, they occur at $\lambda = 1301.9$ and 1318.5 nm, and for TE scattering they occur at $\lambda = 1311.7$ and 1327.3 nm. Using the first three terms of Eq. (1) in [36], their wavelengths are consistent with the partial wavenumbers $n = 57$, 56, respectively, and the radial mode $l = 10$. In Fig. 4, both resonances are noticeably enhanced when θ is in the vicinity of +120° and −120°. This angularly localized enhancement of the MDR intensity is due to constructive interference with the edge ray geometrical resonance. In Fig. 5, the noticeable enhancement reaches its maximum at about +100° and −140°. Both of these enhancements are shifted by about −20° from the predicted scattering angles of the geometrical resonance. This shift is again likely due to a relative phase difference of the scattered MDR field and the scattered geometrical resonance field.

Last, the narrow vertical features at 1304.11 and 1320.22 nm in Figs. 4(a) and 4(b) are additional narrow linewidth TM MDRs, and the narrow features at 1310.9, 1314.61, and 1327.45 nm in Figs. 5(a) and 5(b) are additional narrow linewidth TE MDRs.

5. Conclusion

In this paper, we predicted the observation of enhancements in the elastically scattered MDR intensity from microsphere resonators due to constructive interference with geometrical resonances of rays in the edge region. We also presented numerical simulations demonstrating this effect for the case where the edge of the microsphere is illuminated by an off-axis Gaussian beam. This scattering enhancement can be used as a novel experimental/design parameter for microsphere-based optical applications. This enhancement could possibly be utilized in microsphere biosensors since the additional parameter, i.e., the scattering angle dependence, should lead to increased sensitivity for the detection and analysis of biological agents. The enhancement can also lead to the development of highly sensitive optical sensors and thus finer measurement capability. The plausibility of this novel photonic method in future applications is supported here by our GLMT numerical simulations. The results of Figs. 4 and 5 present physical insights for the design and optimization of

sensors utilizing geometrical-resonance-enhanced MDRs and therefore hold promise for enhancing sensor performance and efficiency.

We would like to thank Türkiye Bilimsel ve Teknolojik Araştırma Kurumu (TÜBİTAK), grant EEEAG-106E215, and the European Commission (EC), grants FP6-IST-003887 NEMO and FP6-IST-511616 PHOREMOST, for the partial support of this research.

References

1. A., Serpengüzel and A. W. Poon, eds., *Optical Processes in Microparticles and Nanostructures* (World Scientific, 2011).
2. A. A. Savchenkov, V. S. Ilchenko, A. B. Matsko, and L. Maleki, "Kilohertz optical resonances in dielectric crystal cavities," Phys. Rev. A **70**, 051804(R) (2004).
3. M. Cai, O. Painter, and K. J. Vahala, "Fiber-coupled microsphere laser," Opt. Lett. **25**, 1430–1432 (2000).
4. T. Bilici, S. Işçi, A. Kurt, and A. Serpengüzel, "Microsphere-based channel dropping filter with an integrated photodetector," IEEE Photon. Technol. Lett. **16**, 476–478 (2004).
5. H. C. Tapalian, J. P. Laine, and P. A. Lane, "Thermooptical switches using coated microsphere resonators," IEEE Photon. Technol. Lett. **14**, 1118–1120 (2002).
6. I. Teraoka, S. Arnold, and F. Vollmer, "Perturbation approach to resonance shifts of whispering-gallery modes in a dielectric microsphere as a probe of a surrounding medium," J. Opt. Soc. Am. B **20**, 1937–1946 (2003).
7. A. Demir and A. Serpengüzel, "Silica microspheres for biomolecular detection applications," IEE Proc. Nanobiotechnol. **152**, 105–108 (2005).
8. A. B. Matsko, A. A. Savchenkov, V. S. Ilchenko, and L. Maleki, "Optical gyroscope with whispering gallery mode optical cavities," Opt. Commun. **233**, 107–112 (2004).
9. R. K., Chang and A. J. Campillo, eds., *Optical Processes in Microcavities* (World Scientific, 1996).
10. G. Gilardi, D. Donisi, A. Serpengüzel, and R. Beccherelli, "Liquid-crystal tunable filter based on sapphire microspheres," Opt. Lett. **34**, 3253–3255 (2009).
11. S. M. Spillane, J. T. Kippenberg, and K. J. Vahala, "Ultralow threshold Raman laser using a spherical dielectric microcavity," Nature **415**, 621–623 (2002).
12. Y. O. Yilmaz, A. Demir, A. Kurt, and A. Serpengüzel, "Optical channel dropping with a silicon microsphere," IEEE Photon. Technol. Lett. **17**, 1662–1664 (2005).
13. A. Serpengüzel, A. Kurt, and U. K. Ayaz, "Silicon microspheres for electronic and photonic integration," Photon. Nanostr. Fundam. Appl. **6**, 179–182 (2008).
14. A. Serpengüzel and A. Demir, "Silicon microspheres for near-IR communication applications," Semicond. Sci. Technol. **23**, 064009 (2008).
15. E. Yüce, O. Gürlü, and A. Serpengüzel, "Optical modulation with silicon microspheres," IEEE Photon. Technol. Lett. **21**, 1481–1483 (2009).
16. F. Vollmer and S. Arnold, "Whispering-gallery-mode biosensing: label-free detection down to single molecules," Nat. Methods **5**, 591–596 (2008).
17. S. Arnold, M. Khoshsima, I. Teraoka, S. Holler, and F. Vollmer, "Shift of whispering-gallery modes in microspheres by protein adsorption," Opt. Lett. **28**, 272–274 (2003).
18. H. C. Ren, F. Vollmer, S. Arnold, and A. Libchaber, "High-*Q* microsphere biosensor—analysis for adsorption of rodlike bacteria," Opt. Express **15**, 17410–17423 (2007).
19. O. Gaathon, J. Culic-Viskota, M. Mihnev, I. Teraoka, and S. Arnold, "Enhancing sensitivity of a whispering gallery mode biosensor by subwavelength confinement," Appl. Phys. Lett. **89**, 223901 (2006).
20. N. Lin, L. Jiang, S. Wang, L. Yuan, H. Xiao, Y. Lu, and H. Tsai, "Ultrasensitive chemical sensors based on whispering gallery modes in a microsphere coated with zeolite," Appl. Opt. **49**, 6463–6471 (2010).
21. J. A. Lock, S. Y. Wrbanek, and K. E. Weiland, "Scattering of a tightly focused beam by optically trapped particle," Appl. Opt. **45**, 3634–3645 (2006).
22. G. Gouesbet, "Generalized Lorenz–Mie theories, the third decade: a perspective," J. Quant. Spectrosc. Radiat. Transfer **110**, 1223–1238 (2009).
23. J. A. Lock and G. Gouesbet, "Generalized Lorenz–Mie theory and applications," J. Quant. Spectrosc. Radiat. Transfer **110**, 800–807 (2009).
24. G. Gouesbet, J. A. Lock, and G. Gréhan, "Generalized Lorenz–Mie theories and description of electromagnetic arbitrary shaped beams: localized approximations and localized beam models, a review," J. Quant. Spectrosc. Radiat. Transfer **112**, 1–27 (2011).
25. G. Griffel, S. Arnold, D. Taskent, A. Serpengüzel, J. Connolly, and N. Morris, "Morphology-dependent resonances of a microsphere-optical fiber system," Opt. Lett. **21**, 695–697 (1996).
26. J. A. Lock, "Excitation efficiency of a morphology-dependent resonance by a focused Gaussian beam," J. Opt. Soc. Am. A **15**, 2986–2994 (1998).
27. H.-B. Lin, J. D. Eversole, A. J. Campillo, and J. P. Barton, "Excitation localization principle for spherical cavities," Opt. Lett. **23**, 1921–1923 (1998).
28. J. A. Lock, "Excitation of morphology-dependent resonances and van de Hulst's localization principle," Opt. Lett. **24**, 427–429 (1999).
29. A. Braun, C. Kornmessser, and V. Beushausen, "Simultaneous spatial and spectral imaging of lasing droplets," J. Opt. Soc. Am. A **22**, 1772–1779 (2005).
30. H. M. Nussenzveig, "High-frequency scattering by a transparent sphere. II. Theory of the rainbow and the glory," J. Math. Phys. **10**, 125–176 (1969).
31. H. M. Nussenzveig, "Complex angular momentum theory of the rainbow and the glory," J. Opt. Soc. Am. **69**, 1068–1079 (1979).
32. G. Gouesbet, S. Meunier-Guttin-Cluzel, and G. Gréhan, "Periodic orbits in Hamiltonian chaos of the annular billiard," Phys. Rev. E **65**, 016212 (2001).
33. J. U. Nöckel and A. D. Stone, "Chaotic light: a theory of asymmetric resonant cavities," in *Optical Processes in Microcavities*, R. K., Chang and A. J. Campillo, eds. (World Scientific, 1996), pp. 389–426.
34. J. A. Lock, "Contribution of high-order rainbows to the scattering of a Gaussian laser beam by a spherical particle," J. Opt. Soc. Am. A **10**, 693–706 (1993).
35. J. A. Lock, "Improved Gaussian beam-scattering algorithm," Appl. Opt. **34**, 559–570 (1995).
36. C. C. Lam, P. T. Leung, and K. Young, "Explicit asymptotic formulas for the positions, widths, and strengths of resonances in Mie scattering," J. Opt. Soc. Am. B **9**, 1585–1592 (1992).